



Article

Enhancement of Sphingomyelinase-Induced Endothelial Nitric Oxide Synthase-Mediated Vasorelaxation in a Murine Model of Type 2 Diabetes

Éva Ruisanchez ^{1,2,†} , Anna Janovicz ^{1,2,†}, Rita Cecília Panta ¹, Levente Kiss ³ , Adrienn Párkányi ¹, Zsuzsa Straky ¹, Dávid Korda ¹, Károly Liliom ⁴ , Gábor Tigyi ^{1,5} and Zoltán Benyó ^{1,2,*}

¹ Institute of Translational Medicine, Semmelweis University, H-1094 Budapest, Hungary

² Eötvös Loránd Research Network and Semmelweis University (ELKH-SE) Cerebrovascular and Neurocognitive Disorders Research Group, H-1052 Budapest, Hungary

³ Department of Physiology, Semmelweis University, H-1094 Budapest, Hungary

⁴ Institute of Biophysics and Radiation Biology, Semmelweis University, H-1094 Budapest, Hungary

⁵ Department of Physiology, University of Tennessee Health Science Center, Memphis, TN 38163, USA

* Correspondence: benyo.zoltan@med.semmelweis-univ.hu

† These authors contributed equally to this work.

Abstract: Sphingolipids are important biological mediators both in health and disease. We investigated the vascular effects of enhanced sphingomyelinase (SMase) activity in a mouse model of type 2 diabetes mellitus (T2DM) to gain an understanding of the signaling pathways involved. Myography was used to measure changes in the tone of the thoracic aorta after administration of 0.2 U/mL neutral SMase in the presence or absence of the thromboxane prostanoid (TP) receptor antagonist SQ 29,548 and the nitric oxide synthase (NOS) inhibitor L-NAME. In precontracted aortic segments of non-diabetic mice, SMase induced transient contraction and subsequent weak relaxation, whereas vessels of diabetic (*Lepr^{db}/Lepr^{db}*, referred to as db/db) mice showed marked relaxation. In the presence of the TP receptor antagonist, SMase induced enhanced relaxation in both groups, which was 3-fold stronger in the vessels of db/db mice as compared to controls and could not be abolished by ceramidase or sphingosine-kinase inhibitors. Co-administration of the NOS inhibitor L-NAME abolished vasorelaxation in both groups. Our results indicate dual vasoactive effects of SMase: TP-mediated vasoconstriction and NO-mediated vasorelaxation. Surprisingly, in spite of the general endothelial dysfunction in T2DM, the endothelial NOS-mediated vasorelaxant effect of SMase was markedly enhanced.

Keywords: sphingolipids; sphingomyelinase; vasorelaxation; endothelial nitric oxide synthase; type 2 diabetes; thromboxane prostanoid receptor



Citation: Ruisanchez, É.; Janovicz, A.; Panta, R.C.; Kiss, L.; Párkányi, A.; Straky, Z.; Korda, D.; Liliom, K.; Tigyi, G.; Benyó, Z. Enhancement of Sphingomyelinase-Induced Endothelial Nitric Oxide Synthase-Mediated Vasorelaxation in a Murine Model of Type 2 Diabetes. *Int. J. Mol. Sci.* **2023**, *24*, 8375. <https://doi.org/10.3390/ijms24098375>

Academic Editors: Simona Gabriela Bungau and Cosmin Mihai Vesa

Received: 28 February 2023

Revised: 30 April 2023

Accepted: 4 May 2023

Published: 6 May 2023



Copyright: © 2023 by the authors. Licensee MDPI, Basel, Switzerland. This article is an open access article distributed under the terms and conditions of the Creative Commons Attribution (CC BY) license (<https://creativecommons.org/licenses/by/4.0/>).

1. Introduction

Sphingolipids, derived from sphingomyelin metabolism, have been implicated as important mediators in the physiology and pathophysiology of the cardiovascular system [1–6]. Sphingomyelinase (SMase) catalyzes the conversion of sphingomyelin to ceramide, which is the precursor of other sphingolipid mediators, including ceramide-1-phosphate (C1P), sphingosine (Sph), and sphingosine-1-phosphate (S1P) [7]. The majority of S1P-induced biological effects are mediated by G-protein-coupled receptors (GPCRs), termed S1P_{1–5} [8]. Other sphingolipid mediators may exert biological effects by directly interacting with membrane or intracellular protein targets, independently of the activation of S1P receptors [5,9–11].

Based on the optimal pH for their catalytic activity, SMase isoforms can be divided into three groups: alkaline, acidic, and neutral [12]. The expression and known functions of alkaline SMases are mostly restricted to the gastrointestinal system, whereas acidic and

neutral SMases are more widely expressed and involved in physiological and pathophysiological reactions in many systems, including the cardiovascular system. In the vasculature, SMases are implicated in the regulation of vascular tone and permeability as well as in causing atherosclerotic lesions and vascular wall remodeling [13]. Interestingly, neutral SMase has been reported to induce a wide range of changes in the vascular tone, depending on the species, vessel type, and experimental conditions (Table 1). Taken into account the large number of biologically active mediators (including ceramides, C1P, Sph, and S1P) that can be generated both extra- and intracellularly upon triggering the sphingolipid biosynthesis by neutral SMase, the diversity of vascular effects is not unexpected.

Table 1. Reported vasoactive effects of neutral SMase.

Species	Vessel	Vasoactive Effects	Proposed Mechanism	Refs.
Yorkshire pig	Coronary artery	Transient endothelium-dependent contraction followed by endothelium-dependent relaxation	Vasoconstriction: prostanoid(s) Vasorelaxation: NO	[14]
Sprague-Dawley rat	Thoracic aorta	Endothelium-independent relaxation	Inhibition of protein kinase C (PKC)	[15,16]
Wistar rat	Thoracic aorta	Partly endothelium-independent relaxation	Endothelium-mediated components are independent of NO or prostanoids Non-endothelial components are independent of PKC	[17]
Mongrel dog	Basilar artery	Endothelium-independent contraction	Activation of VDCC and PKC	[18]
Wistar rat	Pial venule (60–70 μm in diameter)	Constriction and spasm	Activation of VDCC, PKC, and MAP kinase	[19]
Wistar rat	Thoracic aorta	Endothelium-independent relaxation	Inhibition of both Ca^{2+} -dependent and Ca^{2+} -independent (RhoA-/Rho kinase-mediated) contractile pathways	[20]
Cow	Coronary artery	Endothelium-dependent relaxation	Ca^{2+} -independent eNOS activation, involving phosphorylation on serine 1179 and dissociation of eNOS from plasma membrane caveolae	[21]
Wistar rat	Pulmonary artery	Endothelium-independent contraction	Activation of VDCC, PKC ζ , and Rho kinase	[22]
Wistar-Kyoto (WKY) and Spontaneously hypertensive rat (SHR)	Carotid artery	SHR: strong endothelium-dependent contraction WKY: weak endothelium-dependent contraction	Vasoconstriction is mediated by PLA ₂ - and COX2-mediated TXA ₂ release and attenuated by NO	[23–25]

NO, nitric oxide; PKC, protein kinase C; VDCC, voltage-gated calcium channel; MAP, mitogen activated protein; eNOS, endothelial NO synthase; PLA₂, phospholipase A₂; TXA₂, thromboxane A₂; COX, cyclooxygenase.

SMase enzymes are reportedly upregulated in certain cardiovascular and metabolic disorders, such as type 2 diabetes mellitus (T2DM) [13,26,27]. Sphingolipids have been implicated as important regulators of inflammatory processes in diabetes [28]. Stress conditions initiate changes in sphingolipid metabolism [29], and sphingolipids have emerged as key mediators of stress responses [30,31]. Extracellular stressors induce sphingolipid synthesis and turnover, thereby ‘remodeling’ sphingolipid profiles and their topological distribution within cells [32]. Emerging evidence not only demonstrates profound changes in sphingolipid pools and distribution under conditions of overnutrition [33–35], but also implicates sphingolipids in mediating cell-signaling responses that precipitate pathology associated with obesity [36]. In spite of the marked alterations in the metabolism and actions of sphingolipids in diabetes and recent observations indicating that ceramide may contribute to the development of diabetic endothelial dysfunction [37], relatively little is known about the effects of sphingolipids on vascular functions in T2DM. In the present

study, we analyzed the effects of SMase on vascular tone under diabetic conditions in order to elucidate the signaling mechanisms involved.

2. Results

First, we verified the general metabolic and vascular phenotypes of the T2DM mice tested in the present study. Db/db mice reportedly develop obesity with elevated blood glucose levels and insulin resistance [38–40]. Accordingly, the body weight increased almost 2-fold (Figure 1A), whereas blood glucose levels increased 3-fold (Figure 1B) in db/db mice as compared to non-diabetic control littermates. Furthermore, the serum phosphorylcholine level was also significantly increased in the diabetic group (Figure 1C), which is consistent with the reported enhancement of SMase activity in type 2 diabetes [13,26,27]. According to literature data, acetylcholine (ACh)-evoked vasorelaxation of the aorta prepared from db/db mice is completely NOS-dependent [41], thus ACh was used to characterize the endothelial function. The vessels of db/db animals showed marked endothelial dysfunction, as indicated by the impairment of the dose-response relationship of ACh-induced vasorelaxation after precontraction with 10 $\mu\text{mol/L}$ PE (Figure 1D). The E_{max} value decreased to $50.8 \pm 2.0\%$ in diabetic vessels as compared to controls ($65.8 \pm 3.9\%$). However, there was no significant difference in the EC_{50} values (34.7 ± 16.0 nM vs. 55.7 ± 15.7 nM), indicating unchanged potency in spite of the reduced efficacy of endogenous NO upon stimulation of endothelial NOS (eNOS) by ACh. In contrast, reactivity of the vascular smooth muscle to NO remained unaltered, as neither the E_{max} ($105.2 \pm 1.8\%$ vs. $103.3 \pm 2.2\%$) nor the EC_{50} (10.7 ± 1.3 nM vs. 14.1 ± 2.0 nM) values of sodium nitroprusside (SNP)-induced vasorelaxation differed in vessels of db/db animals as compared to controls (Figure 1E). Taken together, these results confirm the T2DM-like metabolic and vascular phenotypes in db/db mice and suggest the in vivo enhancement of SMase activity as well.

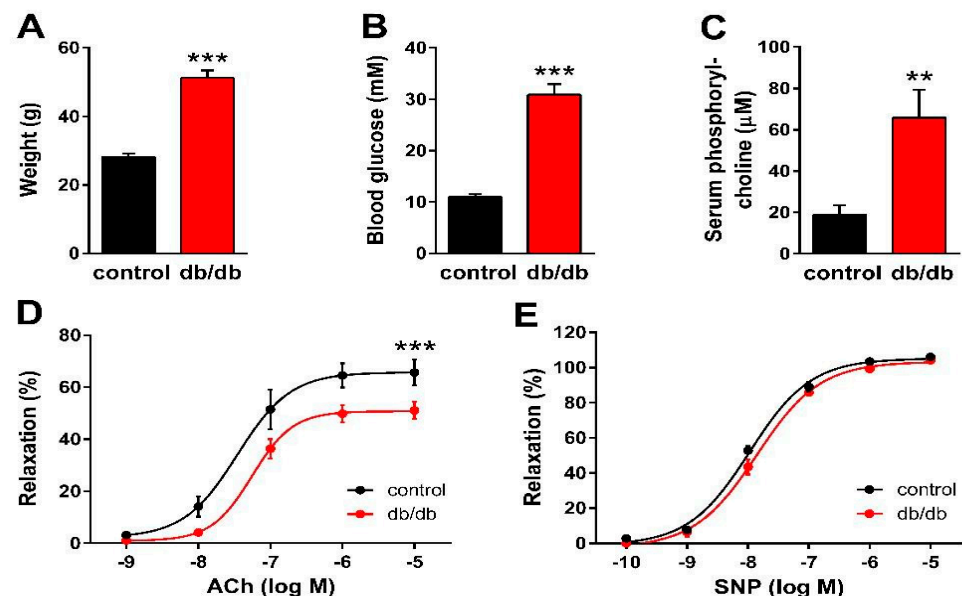


Figure 1. Manifestation of the metabolic and vascular phenotypes of T2DM in db/db mice. Body weight (A), as well as non-fasting blood glucose (B) and serum phosphorylcholine levels (C), increased in db/db mice as compared to controls (** $p < 0.01$, *** $p < 0.001$ vs. control group; Student's unpaired t -test, $n = 13$ –22). ACh-induced relaxation diminished (D), while the reactivity of the vascular smooth muscle to sodium nitroprusside (SNP) remained unaltered (E) in vessels of db/db mice as compared to controls (mean \pm SEM, *** $p < 0.001$ vs. control; dose-response curve fitted to $n = 12$ –24).

Next, we determined the effect of nSMase on the active tone of control and db/db vessels (Figure 2A). After 10 $\mu\text{mol/L}$ phenylephrine (PE)-induced precontraction, 0.2 U/mL nSMase elicited additional contraction in control vessels that reached its maximum at

7.2 min before relaxing back to the pre-SMase level by the end of the 20-min observation period. In contrast, nSMase in db/db vessels elicited completely different responses. After a marked initial relaxation elicited by 0.2 U/mL nSMase during the first 5 min, the tone of the db/db vessels remained in a relaxed state below the level of the initial tension. From the shape of the tension curve, it appeared that in addition to the overriding relaxation, there was a delayed and transient constriction response with a time course similar to that observed in control vessels, but it was unable to overcome the robust dilatation. Evaluation of the AUC (Figure 2B) and the maximal changes in the vascular tone (Figure 2C) also supported the conclusion that there is a marked difference in the vascular effects of nSMase between control and db/db mice: contraction dominates in the former, whereas the latter is characterized by reduction of the vascular tone.

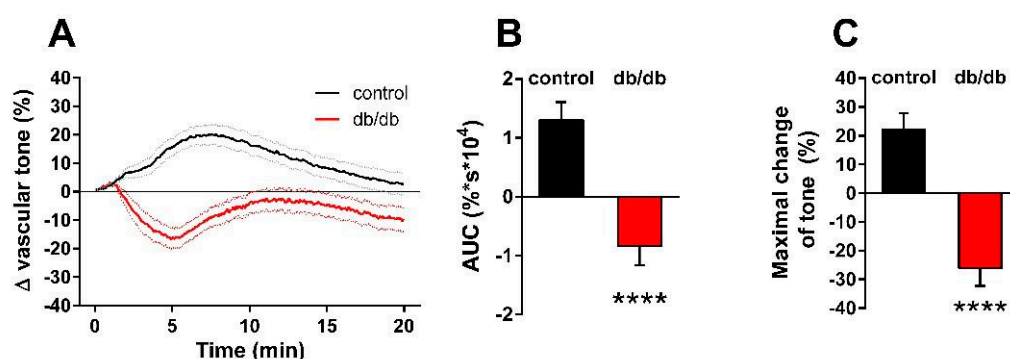


Figure 2. Effects of nSMase on the vascular tone. Application of 0.2 U/mL nSMase evoked a complex vascular effect with dominant contraction in control vessels and a more pronounced relaxation in vessels of db/db mice. Black and red lines on panel (A) represent average changes in tension of PE-precontracted vessels in control and db/db mice, respectively (dotted lines represent SEM). Both area under curve values (B) and maximal tension changes (C) were significantly different in vessels from db/db animals as compared to controls (mean \pm SEM, Student's unpaired *t*-test, **** $p < 0.0001$ vs. control; $n = 51$ –49).

Our next aim was to differentiate the constrictor and relaxant components of the vascular tension changes in response to nSMase. In porcine coronary arteries [14] and in the carotid arteries of spontaneously hypertensive rats [23–25], prostanoids acting on TP receptors have been implicated in mediating the vasoconstrictor effect of SMase. Therefore, we hypothesized that thromboxane prostanoid (TP) receptors also mediate the nSMase-induced vasoconstriction in our murine aorta model. To test this hypothesis, the TP receptor antagonist SQ 29,548 was administered to the organ chambers 30 min prior to administration of nSMase. Blockade of TP receptors not only abolished the vasoconstriction but also converted it to a transient vasorelaxation in control vessels (Figure 3A). The maximum relaxation was reached at 5.5 min after the administration of nSMase, and the vascular tone returned to baseline after 10 min. TP receptor inhibition also markedly changed the vascular response to nSMase in the db/db group: the vasorelaxation was enhanced to more than 70% and reached its maximum at 6.5 min. After its peak, the relaxation decreased, but the vascular tone failed to return to the pre-SMase level even after 20 min. Both the AUC (Figure 3B) and the peak vasorelaxation (Figure 3C) values showed marked differences between the two experimental groups, indicating that the strongly enhanced and prolonged vasorelaxant capacity is responsible for the differences between the vasoactive effects of nSMase in db/db and control vessels. This finding was very surprising in light of the diminished ACh-induced vasorelaxation that we had observed in db/db animals (Figure 1D) and was not consistent with the large body of literature indicating diminished endothelium-dependent vasorelaxation in T2DM.

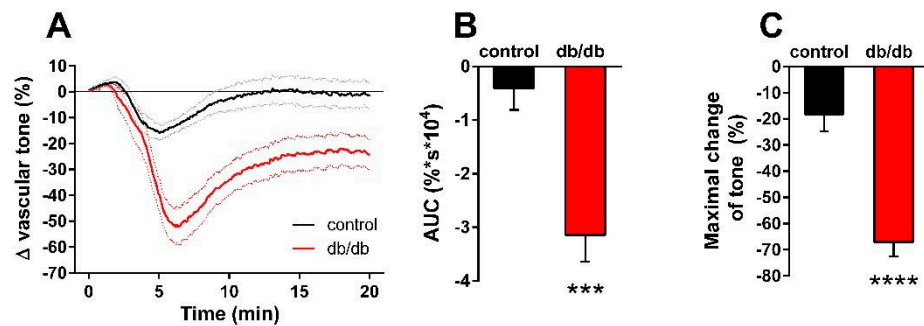


Figure 3. Effects of TP receptor blockade on nSMase-induced changes in the vascular tone. After inhibition of the TP receptor by 1 μ M SQ 29,548, 0.2 U/mL nSMase relaxed both db/db and control vessels, with a significantly higher relaxation in the db/db group (A). Black and red lines in panel A represent average tension changes in PE-precontracted vessels of control and db/db mice, respectively, whereas dotted lines represent SEM. Both area under curve values (B) and maximal tension changes (C) were significantly different in vessels from db/db animals as compared to controls (mean \pm SEM, Student's unpaired *t*-test, *** $p < 0.001$ vs. control; **** $p < 0.0001$ vs. control; $n = 20$).

Next, we aimed to analyze the mechanism of the enhanced nSMase-induced vasorelaxation in the vessels of db/db mice. Theoretically, it could be due to the enhancement of eNOS-mediated vasorelaxation or to the onset of an NO-independent mechanism. To clarify this question, the vessels were incubated with the NOS inhibitor L-NAME (100 μ M) in addition to the TP receptor blocker SQ 29,548 (1 μ M) for 30 min prior to 0.2 U/mL nSMase administration. L-NAME at a concentration of 100 μ M abolished the vasorelaxation observed in the presence of 1 μ M SQ 29,548 both in control and in db/db vessels (Figure 4A). There were no significant differences between the two groups either in the AUC (Figure 4B) or in the maximal change of tension values (Figure 4C). These results indicate that the same secondary signaling pathways—namely TP receptors and eNOS—mediate the vasoactive effects of nSMase in health and in T2DM.

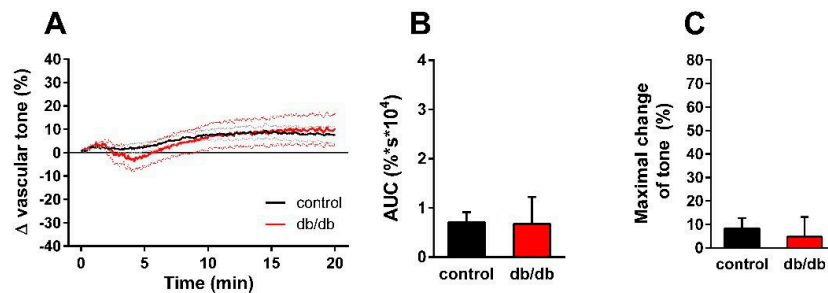


Figure 4. Effects of combined TP receptor and NOS blockade on nSMase-induced changes in vascular tone. After incubation of the vessels with 1 μ M SQ 29,548 and 100 μ M L-NAME for 30 min, 0.2 U/mL nSMase could no longer evoke a tension change in the thoracic aorta of control or db/db mice (A). Black and red lines in panel A represent average tension changes in PE-precontracted vessels of control and db/db mice, respectively (dotted lines represent SEM). Area under curve values (B) and maximal tension changes (C) were not different in vessels from db/db animals as compared to controls (mean \pm SEM, $n = 9$ –17).

Finally, we aimed to investigate the possible involvement of downstream sphingolipid metabolites in the vasorelaxing effect of nSMase observed in db/db mice. Thus, aortic segments isolated from db/db were treated with either the ceramidase inhibitor D-erythro MAPP (10 μ M) or SKI-II (1 μ M), a sphingosine kinase inhibitor. In order to examine the vasorelaxant effects exclusively, vessels were pre-treated with 1 μ M SQ 29,568. Neither MAPP nor SKI-II could affect the vasorelaxation evoked by 0.2 U/mL nSMase (Figure 5A). In addition, evaluation of AUC (Figure 5B) and maximal vasorelaxing responses (Figure 5C) showed no significant differences in MAPP or SKI-II-treated vessels compared to vehicle

treated ones. These results suggest that the effect of nSMase is not mediated by sphingosine or sphingosine-1-phosphate.

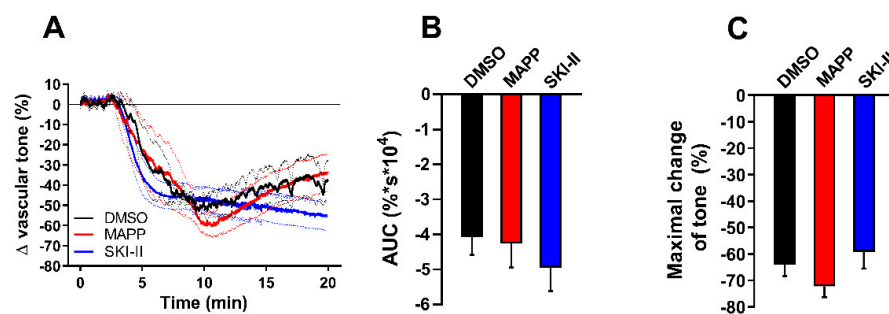


Figure 5. Effects of ceramidase and sphingosine-kinase inhibitors on nSMase-induced vascular tone changes in db/db mice. After incubating with 1 μ M SQ 29,548 for 30 min, db/db vessels were treated with 10 μ M D-erythro MAPP or 1 μ M SKI-II. Neither MAPP nor SKI-II could affect the vasorelaxation induced by 0.2 U/mL nSMase (A). Black, red, and blue lines in panel A represent average tension changes in PE-precontracted vessels of vehicles, MAPP, and SKI-II treated vessels, respectively (dotted lines represent SEM). Area under curve values (B) and maximal tension changes (C) were not different in MAPP- or SKI-II-treated vessels as compared to vehicle controls (mean \pm SEM, $n = 4$ –5).

3. Discussion

Findings of the present study indicate that nSMase-induced changes in vascular tension involve both vasoconstriction and vasorelaxation in murine vessels. Our results suggest that the former is mediated by the release of prostanoids and activation of TP receptors, whereas the latter is mediated by eNOS. Surprisingly, nSMase-induced eNOS-mediated vasorelaxation is markedly enhanced in the vessels of db/db mice in spite of the endothelial dysfunction indicated by the diminished vasorelaxation evoked by ACh. Therefore, nSMase appears to be able to induce enhanced NO release from endothelial cells in T2DM.

Vasoconstriction in response to SMase has been reported in a number of studies, although the mechanisms mediating this effect appear to be highly variable depending on the experimental conditions, including species, vascular region, and integrity of the endothelium (see Table 1). Release of prostanoids and consequent activation of TP receptors have been proposed in porcine coronary arteries [14] as well as in the carotid arteries of spontaneously hypertensive rats [23–25]. In our study, nSMase-induced contraction was found to be TP receptor-dependent in both control and db/db mice, indicating that nSMase stimulates the release of TXA₂ from the aortic rings.

There might be at least three different sources for the SMase-induced arachidonic acid formation necessary for TXA₂ production [42]. One such possibility is that diacylglycerol (DAG) would accumulate while sphingomyelin synthase converted the newly generated ceramide back to sphingomyelin, and DAG lipases would provide arachidonic acid for the production of TXA₂ [43]. Another mechanism might relate to the observation that C1P can allosterically activate phospholipase A₂ (PLA₂) [44], which leads to arachidonic acid formation [45]. It might be important in this context that the gene encoding ceramide kinase (CERK) is upregulated in T2DM [46]. Finally, S1P has been reported recently to regulate prostanoid production in a S1P receptor-dependent manner [47]. It should be noted that mechanisms other than prostanoid release might also mediate the vasoconstrictor effect of SMase, i.e., modulation of different ion channels or initiating the Rho signaling pathway [18,19,22,48].

Vasorelaxation in response to nSMase appears to be endothelial NO-dependent, as L-NAME completely abolished the decrease in vascular tone in both control and db/db vessels. Without L-NAME, relaxation was dramatically increased in db/db-derived vascular rings. This is unexpected because endothelial dysfunction with consequential decreased

vasorelaxant capacity is considered to be a hallmark of T2DM-like conditions. A potential explanation may be related to the altered structure of the plasma membrane in T2DM [49]. Normally, sphingomyelin (SM) represents about 10–20% of the lipids in the plasma membrane, mostly residing in the outer leaflet. However, most of these are found in the caveolae, and SMase is thought to be a regulator of lipid microdomains [50,51]. Pilarczyk and colleagues provided evidence that in db/db mice, the endothelial lining of the aorta contains 10-fold larger lipid raft areas enriched in SM as compared to controls [49]. This arrangement might be related to the decreased NO-release in T2DM, as eNOS is inhibited by caveolin-1 [52], which is considered to be an important regulator of eNOS [53–55]. In our experimental setting, nSMase-induced degradation of sphingomyelin could interfere with this caveolar structure and induce the detachment of eNOS from caveolin-1, leading to high amounts of NO released from the endothelium of db/db vascular rings. This hypothesis is supported by the observations of Mogami et al. [21], indicating that SMase causes endothelium-dependent vasorelaxation through Ca^{2+} -independent endothelial NO production in bovine aortic valves and coronary arteries. They also reported SMase-induced translocation of endothelial NOS from plasma membrane caveolae to the intracellular region. Furthermore, protein expression levels of caveolin-1 were reported to be significantly higher in the aorta of db/db mice, and this was thought to be related to the impaired aortic relaxation of C57BL/KsJ mice [56]. In order to find out if downstream sphingolipid mediators such as sphingosine or sphingosine-1-phosphate contribute to the enhanced vasorelaxation seen in db/db aortic segments, we also investigated whether inhibition of ceramidase or sphingosine-kinase could interfere with the vasorelaxation. Neither D-erythro-MAPP nor SKI-II could diminish the nSMase-induced vasorelaxation in db/db vessels; therefore, it is unlikely that the release of these mediators participates in the effect. This finding strengthens our hypothesis that the enhanced relaxation in db/db vessels is mediated by a direct effect of nSMase on the membrane structure. On the other hand, we cannot rule out that the ceramide-related pathway might be involved in the SMase-induced contractions as well [18,23], as we did not address this question in our experiments. Finally, the potentially increased NO-sensitivity of guanylate cyclase (sGC) [57], which could be related to the dysfunctional NO-release observed in T2DM, should also be considered, as this would sensitize sGC to NO and result in enhanced NO-mediated vasorelaxation. However, this mechanism can be excluded in our present experiments, as the SNP dose-response curve remained unchanged in db/db vessels (Figure 1E), indicating that the sensitivity of the vascular smooth muscle to NO was not upregulated.

Sphingolipid metabolism is markedly altered in T2DM and related conditions [58–62], and the observed changes in endothelial lipid rafts [49] might be a consequence of the disrupted plasma membrane lipid metabolism. On the other hand, T2DM has several characteristics that resemble a chronic inflammatory disease [63]. Cytokines that accumulate in chronic inflammation, such as tumor necrosis factor alpha (TNF- α) and interleukin 1 beta (IL-1 β), can also induce marked changes in sphingolipid metabolism [6,64,65]. Our observation that serum phosphorylcholine levels were increased in the db/db group might be a strong indicator of the altered in vivo sphingolipid metabolism in our animal model and agrees with the literature; however, it cannot be excluded that enzymes other than nSMase also contribute to this increase (e.g., other SMases, choline-kinase, phospholipase C, ENPP, etc.).

As a limitation of our study, it has to be mentioned that the characteristics of the pathophysiological conditions in the db/db mouse model differ from those of human T2DM in some aspects [66]. For example, db/db mice do not necessarily develop hypertension and may have high levels of high-density lipoprotein and a reduced tendency toward atherosclerosis [67]. Therefore, due to the more severe endothelial dysfunction, the enhancement of nSMase-induced eNOS-mediated vasorelaxation may be limited in humans with T2DM. A further limitation of our study is that we tested only one single dose of bacterial nSMase. This 0.2 U/mL dose of exogenously administered bacterial nSMase represents the upper range used in the literature [14–18,20–23], as our aim was to evaluate the

consequences of a robust activation of sphingomyelinase degradation. Further studies may aim to elucidate the exact dose-response relationship for SMase-induced vasorelaxation and vasoconstriction in db/db mice or other T2DM-related conditions, which may also help to clarify the exact molecular mechanisms involved. Though bacterial and different mammalian nSMase orthologues share low overall homology, the ‘catalytic core’ residues are strongly conserved [68]. Therefore, it is likely that the addition of bacterial nSMase mimics the overactivation of mammalian nSMase and leads to similar cellular effects—in our case, the release of thromboxane and NO [69,70].

4. Materials and Methods

All procedures were carried out according to the guidelines of the Hungarian Law of Animal Protection (40/2013). The procedures were approved by the National Scientific Ethical Committee of Animal Experimentation (PE/EA/924-7/2021, accepted: 7 September 2021).

4.1. Animals and General Procedures

The BKS db diabetic mouse strain (JAX stock #000642) was obtained from the Jackson Laboratory (Bar Harbor, ME, USA) and has been maintained in our animal facility by mating repulsion double heterozygotes (*Dock7^m +/+ Lep^{rdb}*). Littermate adult male diabetic (*Lep^{rdb} / Lep^{rdb}*, referred to as db/db) and misty (*Dock7^m / Dock7^m*, referred to as control) mice were selected for experiments. All mice investigated in this research were male and aged between 90 and 180 days. Animals were weighed, and blood samples were collected by cardiac puncture followed by transcatheter perfusion with 10 mL of heparinized (10 IU/mL) Krebs solution under deep ether anesthesia, as described previously [71]. Nonfasting blood glucose was measured by a Dcont IDEÁL biosensor-type blood glucose meter (77 Elektronika Kft.; Budapest, Hungary). In some experiments, additional blood samples were collected, allowed to clot for 30 min at room temperature, and centrifuged at 2000× *g* for 15 min at 4 °C. Serum was snap frozen for a later phosphorylcholine assay, which was based on the method described by Hojjati and Jiang [72] using a commercially available kit (item No. 10009928, Cayman Chemical; Ann Arbor, MI, USA).

4.2. Myography

The thoracic aorta was removed and cleaned of fat and connective tissue under a dissection microscope (M3Z, Wild Heerbrugg AG; Gais, Switzerland) and immersed in a Krebs solution of the following composition (mmol/L): 119 NaCl, 4.7 KCl, 1.2 KH₂PO₄, 2.5 CaCl₂·2 H₂O, 1.2 MgSO₄·7 H₂O, 20 NaHCO₃, 0.03 EDTA, and 10 glucose at room temperature and pH 7.4. Vessels were cut into ~3 mm-long segments and mounted on stainless steel vessel holders (200 µm in diameter) in a conventional myograph setup (610 M multiwire myograph system; Danish Myo Technology A/S; Aarhus, Denmark). Special care was taken to preserve the endothelium.

The wells of the myographs were filled with an 8 mL Krebs solution aerated with carbogen. The vessels were allowed a 30-min resting period, during which the bath solution was warmed to 37 °C and the passive tension was adjusted to 15 mN, which was determined to be optimal in a previous study [71]. Subsequently, the tissues were exposed to a 124 mmol/L K⁺ Krebs solution (made by isomolar replacement of Na⁺ by K⁺) for 1 min, followed by several washes with normal Krebs solution. Reactivity of the smooth muscle was tested by a contraction evoked by 10 µmol/L PE, and reactivity of the endothelium was tested by following the PE-evoked contraction with administration of 0.1 µmol/L ACh. After repeated washing, during which the vascular tension returned to the resting level, the segments were exposed to a 124 mmol/L K⁺ Krebs solution for 3 min in order to elicit a reference maximal contraction. Subsequently, after a 30-min washout, increasing concentrations of PE (0.1 nmol/L to 10 µmol/L) and ACh (1 nmol/L to 10 µmol/L) were administered to determine the reactivity of the smooth muscle and the endothelium, respectively. Following a 30-min resting period, the vessels were precontracted to 70–90% of the reference contraction by an appropriate concentration of PE, and after contraction

had stabilized, the effects of 0.2 U/mL nSMase (SMase from *B. cereus*, Sigma-Aldrich; St. Louis, MO, USA) were investigated for 20 min. Bacterial SMase functions at neutral pH and is reportedly a useful tool for mimicking the biological effects of activation of cellular SMase [73,74]. In some experiments, the selective TP receptor antagonist SQ 29,548 (1 μ M) with or without the nitric oxide synthase (NOS) inhibitor L-NAME (100 μ M) was applied to the baths 30 min prior to administration of nSMase. In order to block ceramidase or sphingosine-kinase enzymes, D-erythro MAPP (10 μ M) or SKI-II (1 μ M) were used, respectively. Finally, to test the sensitivity of the smooth muscle to NO, SNP (0.1 nmol/L to 10 μ mol/L) was administered after a stable precontraction elicited by 1 μ mol/L PE.

4.3. Data Analysis

An MP100 system and AcqKnowledge 3.72 software from Biopac System Inc. (Goleta, CA, USA) were used to record and analyze changes in the vascular tone. All data are presented as mean \pm SE, and “*n*” indicates the number of vascular segments tested in myography experiments or the number of animals tested in the case of body weight, blood glucose, and serum phosphorylcholine levels. Maximal changes in the vascular tone were calculated as a percentage of precontraction. To evaluate the temporal pattern of nSMase-induced vasoactive responses, individual curves were constructed and averaged, showing the changes in vascular tone for 20 min after the application of nSMase. Area under the curve (AUC) values were calculated from individual experiments for quantification of the overall vasoactive effect. The statistical analysis was performed using the GraphPad Prism software v.6.07 from GraphPad Software Inc. (La Jolla, CA, USA). Student’s unpaired *t*-test was applied when comparing two variables, and a *p* value of less than 0.05 was considered to be statistically significant. The effects of cumulative doses of PE and ACh were evaluated by dose-response curve fitting for the determination of E_{max} and EC_{50} values. All data presented in this study are available in the Supplementary Material File (Figures S1–S5).

4.4. Reagents

All reagents in this study, including nSMase, were purchased from Sigma-Aldrich (St. Louis, MO, USA), except SQ 29,548, which was from Santa Cruz Biotechnology (Dallas, TX, USA).

5. Conclusions

Administration of nSMase induces TP receptor-mediated vasoconstriction and eNOS-mediated vasorelaxation in murine vessels. In spite of endothelial dysfunction in db/db mice, the vasorelaxant effect of nSMase is markedly augmented. SMase-mediated disruption of SM in endothelial lipid rafts might represent a possible mechanism responsible for enhanced NO generation in T2DM. An intriguing interpretation of our finding is that the retraction of eNOS in sphingomyelin-rich microdomains of the endothelial plasma membrane could contribute significantly to the development of vascular dysfunction in T2DM.

Supplementary Materials: The following supporting information can be downloaded at: <https://www.mdpi.com/article/10.3390/ijms24098375/s1>.

Author Contributions: Conceptualization, É.R., L.K., G.T. and Z.B.; methodology, É.R. and Z.B.; validation, K.L., G.T. and Z.B.; investigation, É.R., A.J., R.C.P., A.P., Z.S. and D.K.; resources, Z.B.; data curation, É.R., R.C.P., A.J., A.P., Z.S. and D.K.; writing—original draft preparation, É.R., A.J., L.K., K.L., G.T. and Z.B.; visualization, É.R. and A.J.; supervision, L.K., K.L., G.T. and Z.B.; project administration, Z.B.; funding acquisition, É.R. and Z.B. All authors have read and agreed to the published version of the manuscript.

Funding: This research was funded by the Hungarian National Research, Development, and Innovation Office (OTKA K-112964, K-125174, K-139230, and PD-132851) and by the Ministry of Innovation and Technology of Hungary from the NRD Fund (2020-1.1.6-JÖVŐ-2021-00010, 2020-1.1.6-JÖVŐ-2021-00013 and TKP2021-EGA-25).

Institutional Review Board Statement: The animal experiments were carried out according to the guidelines of the Hungarian Law of Animal Protection (40/2013) and were approved by the National Scientific Ethical Committee of Animal Experimentation (PE_EA_924-7_2021, Approval date: 7 September 2021).

Informed Consent Statement: Not applicable.

Data Availability Statement: The data presented in this study are available in the Supplemental File.

Acknowledgments: The authors are grateful to Margit Kerék for expert technical assistance and to Erzsébet Fejes for critically reading the manuscript.

Conflicts of Interest: The authors declare no conflict of interest. The funders had no role in the design of the study, in the collection, analysis, or interpretation of data, in the writing of the manuscript, or in the decision to publish the results.

References

1. Peters, S.L.; Alewijnse, A.E. Sphingosine-1-phosphate signaling in the cardiovascular system. *Curr. Opin. Pharmacol.* **2007**, *7*, 186–192. [[CrossRef](#)] [[PubMed](#)]
2. Igarashi, J.; Michel, T. Sphingosine-1-phosphate and modulation of vascular tone. *Cardiovasc. Res.* **2009**, *82*, 212–220. [[CrossRef](#)] [[PubMed](#)]
3. Kerage, D.; Brindley, D.N.; Hemmings, D.G. Review: Novel insights into the regulation of vascular tone by sphingosine 1-phosphate. *Placenta* **2014**, *35*, S86–S92. [[CrossRef](#)] [[PubMed](#)]
4. Proia, R.L.; Hla, T. Emerging biology of sphingosine-1-phosphate: Its role in pathogenesis and therapy. *J. Clin. Investig.* **2015**, *125*, 1379–1387. [[CrossRef](#)]
5. Hemmings, D.G. Signal transduction underlying the vascular effects of sphingosine 1-phosphate and sphingosylphosphorylcholine. *Naunyn. Schmiedebergs Arch. Pharmacol.* **2006**, *373*, 18–29. [[CrossRef](#)] [[PubMed](#)]
6. De Palma, C.; Meacci, E.; Perrotta, C.; Bruni, P.; Clementi, E. Endothelial nitric oxide synthase activation by tumor necrosis factor alpha through neutral sphingomyelinase 2, sphingosine kinase 1, and sphingosine 1 phosphate receptors: A novel pathway relevant to the pathophysiology of endothelium. *Arterioscler. Thromb. Vasc. Biol.* **2006**, *26*, 99–105. [[CrossRef](#)] [[PubMed](#)]
7. Fyrst, H.; Saba, J.D. An update on sphingosine-1-phosphate and other sphingolipid mediators. *Nat. Chem. Biol.* **2010**, *6*, 489–497. [[CrossRef](#)] [[PubMed](#)]
8. Meyer zu Heringdorf, D.; Jakobs, K.H. Lysophospholipid receptors: Signalling, pharmacology and regulation by lysophospholipid metabolism. *Biochim. Biophys. Acta* **2007**, *1768*, 923–940. [[CrossRef](#)]
9. Strub, G.M.; Maceyka, M.; Hait, N.C.; Milstien, S.; Spiegel, S. Extracellular and intracellular actions of sphingosine-1-phosphate. *Adv. Exp. Med. Biol.* **2010**, *688*, 141–155.
10. Hla, T.; Dannenberg, A.J. Sphingolipid signaling in metabolic disorders. *Cell Metab.* **2012**, *16*, 420–434. [[CrossRef](#)]
11. Ernst, A.M.; Brugger, B. Sphingolipids as modulators of membrane proteins. *Biochim. Biophys. Acta* **2014**, *1841*, 665–670. [[CrossRef](#)] [[PubMed](#)]
12. Adada, M.; Luberto, C.; Canals, D. Inhibitors of the sphingomyelin cycle: Sphingomyelin synthases and sphingomyelinases. *Chem. Phys. Lipids* **2016**, *197*, 45–59. [[CrossRef](#)]
13. Pavoine, C.; Pecker, F. Sphingomyelinases: Their regulation and roles in cardiovascular pathophysiology. *Cardiovasc. Res.* **2009**, *82*, 175–183. [[CrossRef](#)] [[PubMed](#)]
14. Murohara, T.; Kugiyama, K.; Ohgushi, M.; Sugiyama, S.; Ohta, Y.; Yasue, H. Effects of sphingomyelinase and sphingosine on arterial vasomotor regulation. *J. Lipid Res.* **1996**, *37*, 1601–1608. [[CrossRef](#)] [[PubMed](#)]
15. Johns, D.G.; Jin, J.S.; Wilde, D.W.; Webb, R.C. Ceramide-induced vasorelaxation: An inhibitory action on protein kinase C. *Gen. Pharmacol.* **1999**, *33*, 415–421. [[CrossRef](#)] [[PubMed](#)]
16. Johns, D.G.; Osborn, H.; Webb, R.C. Ceramide: A novel cell signaling mechanism for vasodilation. *Biochem. Biophys. Res. Commun.* **1997**, *237*, 95–97. [[CrossRef](#)]
17. Zheng, T.; Li, W.; Wang, J.; Altura, B.T.; Altura, B.M. Effects of neutral sphingomyelinase on phenylephrine-induced vasoconstriction and Ca(2+) mobilization in rat aortic smooth muscle. *Eur. J. Pharmacol.* **2000**, *391*, 127–135. [[CrossRef](#)]
18. Zheng, T.; Li, W.; Wang, J.; Altura, B.T.; Altura, B.M. Sphingomyelinase and ceramide analogs induce contraction and rises in [Ca(2+)](i) in canine cerebral vascular muscle. *Am. J. Physiol. Heart Circ. Physiol.* **2000**, *278*, H1421–H1428. [[CrossRef](#)] [[PubMed](#)]
19. Altura, B.M.; Gebrewold, A.; Zheng, T.; Altura, B.T. Sphingomyelinase and ceramide analogs induce vasoconstriction and leukocyte-endothelial interactions in cerebral venules in the intact rat brain: Insight into mechanisms and possible relation to brain injury and stroke. *Brain Res. Bull.* **2002**, *58*, 271–278. [[CrossRef](#)]
20. Jang, G.J.; Ahn, D.S.; Cho, Y.E.; Morgan, K.G.; Lee, Y.H. C₂-ceramide induces vasodilation in phenylephrine-induced pre-contracted rat thoracic aorta: Role of RhoA/Rho-kinase and intracellular Ca²⁺ concentration. *Naunyn. Schmiedebergs Arch. Pharmacol.* **2005**, *372*, 242–250. [[CrossRef](#)] [[PubMed](#)]
21. Mogami, K.; Kishi, H.; Kobayashi, S. Sphingomyelinase causes endothelium-dependent vasorelaxation through endothelial nitric oxide production without cytosolic Ca²⁺ elevation. *FEBS Lett.* **2005**, *579*, 393–397. [[CrossRef](#)] [[PubMed](#)]

22. Cogolludo, A.; Moreno, L.; Frazziano, G.; Moral-Sanz, J.; Menendez, C.; Castaneda, J.; Gonzalez, C.; Villamor, E.; Perez-Vizcaino, F. Activation of neutral sphingomyelinase is involved in acute hypoxic pulmonary vasoconstriction. *Cardiovasc. Res.* **2009**, *82*, 296–302. [[CrossRef](#)] [[PubMed](#)]
23. Spijkers, L.J.; van den Akker, R.F.; Janssen, B.J.; Debets, J.J.; De Mey, J.G.; Stroes, E.S.; van den Born, B.J.; Wijesinghe, D.S.; Chalfant, C.E.; MacAleese, L.; et al. Hypertension is associated with marked alterations in sphingolipid biology: A potential role for ceramide. *PLoS ONE* **2011**, *6*, e21817. [[CrossRef](#)] [[PubMed](#)]
24. Spijkers, L.J.; Janssen, B.J.; Nelissen, J.; Meens, M.J.; Wijesinghe, D.; Chalfant, C.E.; De Mey, J.G.; Alewijnse, A.E.; Peters, S.L. Antihypertensive treatment differentially affects vascular sphingolipid biology in spontaneously hypertensive rats. *PLoS ONE* **2011**, *6*, e29222. [[CrossRef](#)] [[PubMed](#)]
25. van den Elsen, L.W.; Spijkers, L.J.; van den Akker, R.F.; van Winssen, A.M.; Balvers, M.; Wijesinghe, D.S.; Chalfant, C.E.; Garssen, J.; Willemsen, L.E.; Alewijnse, A.E.; et al. Dietary fish oil improves endothelial function and lowers blood pressure via suppression of sphingolipid-mediated contractions in spontaneously hypertensive rats. *J. Hypertens.* **2014**, *32*, 1050–1058; discussion 1058. [[CrossRef](#)] [[PubMed](#)]
26. Shamseddine, A.A.; Airola, M.V.; Hannun, Y.A. Roles and regulation of neutral sphingomyelinase-2 in cellular and pathological processes. *Adv. Biol. Regul.* **2015**, *57*, 24–41. [[CrossRef](#)]
27. Russo, S.B.; Ross, J.S.; Cowart, L.A. Sphingolipids in obesity, type 2 diabetes, and metabolic disease. *Handb. Exp. Pharmacol.* **2013**, *216*, 373–401. [[CrossRef](#)]
28. Cowart, L.A. Sphingolipids: Players in the pathology of metabolic disease. *Trends Endocrinol. Metab.* **2009**, *20*, 34–42. [[CrossRef](#)]
29. Hannun, Y.A.; Obeid, L.M. The ceramide-centric universe of lipid-mediated cell regulation: Stress encounters of the lipid kind. *J. Biol. Chem.* **2002**, *277*, 25847–25850. [[CrossRef](#)] [[PubMed](#)]
30. Sawai, H.; Hannun, Y.A. Ceramide and sphingomyelinases in the regulation of stress responses. *Chem. Phys. Lipids* **1999**, *102*, 141–147. [[CrossRef](#)] [[PubMed](#)]
31. Hannun, Y.A.; Luberto, C. Ceramide in the eukaryotic stress response. *Trends Cell Biol.* **2000**, *10*, 73–80. [[CrossRef](#)] [[PubMed](#)]
32. van Meer, G.; Holthuis, J.C. Sphingolipid transport in eukaryotic cells. *Biochim. Biophys. Acta* **2000**, *1486*, 145–170. [[CrossRef](#)] [[PubMed](#)]
33. Holland, W.L.; Summers, S.A. Sphingolipids, insulin resistance, and metabolic disease: New insights from in vivo manipulation of sphingolipid metabolism. *Endocr. Rev.* **2008**, *29*, 381–402. [[CrossRef](#)] [[PubMed](#)]
34. Unger, R.H.; Orci, L. Lipoapoptosis: Its mechanism and its diseases. *Biochim. Biophys. Acta* **2002**, *1585*, 202–212. [[CrossRef](#)]
35. Boden, G. Pathogenesis of type 2 diabetes. Insulin resistance. *Endocrinol. Metab. Clin. N. Am.* **2001**, *30*, 801–815, v. [[CrossRef](#)] [[PubMed](#)]
36. Samad, F. Contribution of sphingolipids to the pathogenesis of obesity. *Future Lipidol.* **2007**, *2*, 625–639. [[CrossRef](#)]
37. Symons, J.D.; Abel, E.D. Lipotoxicity contributes to endothelial dysfunction: A focus on the contribution from ceramide. *Rev. Endocr. Metab. Disord.* **2013**, *14*, 59–68. [[CrossRef](#)]
38. Aasum, E.; Hafstad, A.D.; Severson, D.L.; Larsen, T.S. Age-dependent changes in metabolism, contractile function, and ischemic sensitivity in hearts from db/db mice. *Diabetes* **2003**, *52*, 434–441. [[CrossRef](#)] [[PubMed](#)]
39. Coleman, D.L. Obese and diabetes: Two mutant genes causing diabetes-obesity syndromes in mice. *Diabetologia* **1978**, *14*, 141–148. [[CrossRef](#)] [[PubMed](#)]
40. Do, O.H.; Low, J.T.; Gaisano, H.Y.; Thorn, P. The secretory deficit in islets from db/db mice is mainly due to a loss of responding beta cells. *Diabetologia* **2014**, *57*, 1400–1409. [[CrossRef](#)] [[PubMed](#)]
41. Sallam, N.A.; Laher, I. Redox Signaling and Regional Heterogeneity of Endothelial Dysfunction in db/db Mice. *Int. J. Mol. Sci.* **2020**, *21*, 6147. [[CrossRef](#)]
42. Ramadan, F.M.; Upchurch, G.R., Jr.; Keagy, B.A.; Johnson, G., Jr. Endothelial cell thromboxane production and its inhibition by a calcium-channel blocker. *Ann. Thorac. Surg.* **1990**, *49*, 916–919. [[CrossRef](#)]
43. Epanand, R.M.; So, V.; Jennings, W.; Khadka, B.; Gupta, R.S.; Lemaire, M. Diacylglycerol Kinase-epsilon: Properties and Biological Roles. *Front. Cell. Dev. Biol.* **2016**, *4*, 112. [[CrossRef](#)] [[PubMed](#)]
44. Subramanian, P.; Vora, M.; Gentile, L.B.; Stahelin, R.V.; Chalfant, C.E. Anionic lipids activate group IVA cytosolic phospholipase A2 via distinct and separate mechanisms. *J. Lipid Res.* **2007**, *48*, 2701–2708. [[CrossRef](#)] [[PubMed](#)]
45. Pettus, B.J.; Bielawska, A.; Spiegel, S.; Roddy, P.; Hannun, Y.A.; Chalfant, C.E. Ceramide kinase mediates cytokine- and calcium ionophore-induced arachidonic acid release. *J. Biol. Chem.* **2003**, *278*, 38206–38213. [[CrossRef](#)] [[PubMed](#)]
46. Mitsutake, S.; Date, T.; Yokota, H.; Sugiura, M.; Kohama, T.; Igarashi, Y. Ceramide kinase deficiency improves diet-induced obesity and insulin resistance. *FEBS Lett.* **2012**, *586*, 1300–1305. [[CrossRef](#)] [[PubMed](#)]
47. Machida, T.; Matamura, R.; Iizuka, K.; Hirafuji, M. Cellular function and signaling pathways of vascular smooth muscle cells modulated by sphingosine 1-phosphate. *J. Pharmacol. Sci.* **2016**, *132*, 211–217. [[CrossRef](#)] [[PubMed](#)]
48. Goto, K.; Kitazono, T. Endothelium-dependent hyperpolarization (EDH) in diet-induced obesity. *Endocr. Metab. Sci.* **2020**, *1*, 100062. [[CrossRef](#)]
49. Pilarczyk, M.; Mateuszuk, L.; Rygula, A.; Kepczynski, M.; Chlopicki, S.; Baranska, M.; Kaczor, A. Endothelium in spots—high-content imaging of lipid rafts clusters in db/db mice. *PLoS ONE* **2014**, *9*, e106065. [[CrossRef](#)]

50. Mitsutake, S.; Zama, K.; Yokota, H.; Yoshida, T.; Tanaka, M.; Mitsui, M.; Ikawa, M.; Okabe, M.; Tanaka, Y.; Yamashita, T.; et al. Dynamic modification of sphingomyelin in lipid microdomains controls development of obesity, fatty liver, and type 2 diabetes. *J. Biol. Chem.* **2011**, *286*, 28544–28555. [[CrossRef](#)] [[PubMed](#)]
51. Romiti, E.; Meacci, E.; Tanzi, G.; Becciolini, L.; Mitsutake, S.; Farnararo, M.; Ito, M.; Bruni, P. Localization of neutral ceramidase in caveolin-enriched light membranes of murine endothelial cells. *FEBS Lett.* **2001**, *506*, 163–168. [[CrossRef](#)] [[PubMed](#)]
52. Jasmin, J.F.; Frank, P.G.; Lisanti, M.P. Caveolins and caveolae: Roles in signaling and disease mechanism. In *Advances in Experimental Medicine and Biology*; Springer Science + Business Media, LCC.: New York, NY, USA, 2012; pp. 3–13.
53. Garcia-Cardena, G.; Martasek, P.; Masters, B.S.; Skidd, P.M.; Couet, J.; Li, S.; Lisanti, M.P.; Sessa, W.C. Dissecting the interaction between nitric oxide synthase (NOS) and caveolin. Functional significance of the nos caveolin binding domain in vivo. *J. Biol. Chem.* **1997**, *272*, 25437–25440. [[CrossRef](#)] [[PubMed](#)]
54. Frank, P.G.; Woodman, S.E.; Park, D.S.; Lisanti, M.P. Caveolin, caveolae, and endothelial cell function. *Arterioscler. Thromb. Vasc. Biol.* **2003**, *23*, 1161–1168. [[CrossRef](#)] [[PubMed](#)]
55. Shaul, P.W. Regulation of endothelial nitric oxide synthase: Location, location, location. *Annu. Rev. Physiol.* **2002**, *64*, 749–774. [[CrossRef](#)]
56. Lam, T.Y.; Seto, S.W.; Lau, Y.M.; Au, L.S.; Kwan, Y.W.; Ngai, S.M.; Tsui, K.W. Impairment of the vascular relaxation and differential expression of caveolin-1 of the aorta of diabetic +db/+db mice. *Eur. J. Pharmacol.* **2006**, *546*, 134–141. [[CrossRef](#)]
57. Miller, M.A.; Morgan, R.J.; Thompson, C.S.; Mikhailidis, D.P.; Jeremy, J.Y. Adenylate and guanylate cyclase activity in the penis and aorta of the diabetic rat: An in vitro study. *Br. J. Urol.* **1994**, *74*, 106–111. [[CrossRef](#)]
58. Samad, F.; Hester, K.D.; Yang, G.; Hannun, Y.A.; Bielawski, J. Altered adipose and plasma sphingolipid metabolism in obesity: A potential mechanism for cardiovascular and metabolic risk. *Diabetes* **2006**, *55*, 2579–2587. [[CrossRef](#)]
59. Arora, T.; Velagapudi, V.; Pournaras, D.J.; Welbourn, R.; le Roux, C.W.; Oresic, M.; Backhed, F. Roux-en-Y gastric bypass surgery induces early plasma metabolomic and lipidomic alterations in humans associated with diabetes remission. *PLoS ONE* **2015**, *10*, e0126401. [[CrossRef](#)]
60. Fox, T.E.; Bewley, M.C.; Unrath, K.A.; Pedersen, M.M.; Anderson, R.E.; Jung, D.Y.; Jefferson, L.S.; Kim, J.K.; Bronson, S.K.; Flanagan, J.M.; et al. Circulating sphingolipid biomarkers in models of type 1 diabetes. *J. Lipid Res.* **2011**, *52*, 509–517. [[CrossRef](#)]
61. Gorska, M.; Baranczuk, E.; Dobrzyn, A. Secretory Zn²⁺-dependent sphingomyelinase activity in the serum of patients with type 2 diabetes is elevated. *Horm. Metab. Res.* **2003**, *35*, 506–507. [[CrossRef](#)]
62. Gorska, M.; Dobrzyn, A.; Baranowski, M. Concentrations of sphingosine and sphinganine in plasma of patients with type 2 diabetes. *Med. Sci. Monit.* **2005**, *11*, CR35–CR38. [[PubMed](#)]
63. Donath, M.Y.; Shoelson, S.E. Type 2 diabetes as an inflammatory disease. *Nat. Rev. Immunol.* **2011**, *11*, 98–107. [[CrossRef](#)] [[PubMed](#)]
64. Dressler, K.A.; Mathias, S.; Kolesnick, R.N. Tumor necrosis factor- α activates the sphingomyelin signal transduction pathway in a cell-free system. *Science* **1992**, *255*, 1715–1718. [[CrossRef](#)] [[PubMed](#)]
65. Wiegmann, K.; Schutze, S.; Machleidt, T.; Witte, D.; Kronke, M. Functional dichotomy of neutral and acidic sphingomyelinases in tumor necrosis factor signaling. *Cell* **1994**, *78*, 1005–1015. [[CrossRef](#)] [[PubMed](#)]
66. Wang, B.; Chandrasekera, P.C.; Pippin, J.J. Leptin- and leptin receptor-deficient rodent models: Relevance for human type 2 diabetes. *Curr. Diabetes Rev.* **2014**, *10*, 131–145. [[CrossRef](#)]
67. Cohen, M.P.; Clements, R.S.; Hud, E.; Cohen, J.A.; Ziyadeh, F.N. Evolution of renal function abnormalities in the db/db mouse that parallels the development of human diabetic nephropathy. *Exp. Nephrol.* **1996**, *4*, 166–171.
68. Clarke, C.J.; Snook, C.F.; Tani, M.; Matmati, N.; Marchesini, N.; Hannun, Y.A. The extended family of neutral sphingomyelinases. *Biochemistry* **2006**, *45*, 11247–11256. [[CrossRef](#)]
69. Schulz, M.K.; Gutterman, D.K.; Freed, J.K. Activation of Neutral Sphingomyelinase Contributes to Nitric Oxide-Mediated Flow-Induced Dilation in the Human Microvasculature. *FASEB J.* **2020**, *34*, 1. [[CrossRef](#)]
70. Bautista-Perez, R.; del Valle-Mondragon, L.; Cano-Martinez, A.; Perez-Mendez, O.; Escalante, B.; Franco, M. Involvement of neutral sphingomyelinase in the angiotensin II signaling pathway. *Am. J. Physiol. Renal. Physiol.* **2015**, *308*, F1178–F1187. [[CrossRef](#)]
71. Horvath, B.; Orsy, P.; Benyo, Z. Endothelial NOS-mediated relaxations of isolated thoracic aorta of the C57BL/6J mouse: A methodological study. *J. Cardiovasc. Pharmacol.* **2005**, *45*, 225–231. [[CrossRef](#)]
72. Hojjati, M.R.; Jiang, X.C. Rapid, specific, and sensitive measurements of plasma sphingomyelin and phosphatidylcholine. *J. Lipid Res.* **2006**, *47*, 673–676. [[CrossRef](#)] [[PubMed](#)]
73. Raines, M.A.; Kolesnick, R.N.; Golde, D.W. Sphingomyelinase and ceramide activate mitogen-activated protein kinase in myeloid HL-60 cells. *J. Biol. Chem.* **1993**, *268*, 14572–14575. [[CrossRef](#)] [[PubMed](#)]
74. Linardic, C.M.; Hannun, Y.A. Identification of a distinct pool of sphingomyelin involved in the sphingomyelin cycle. *J. Biol. Chem.* **1994**, *269*, 23530–23537. [[CrossRef](#)] [[PubMed](#)]

Disclaimer/Publisher’s Note: The statements, opinions and data contained in all publications are solely those of the individual author(s) and contributor(s) and not of MDPI and/or the editor(s). MDPI and/or the editor(s) disclaim responsibility for any injury to people or property resulting from any ideas, methods, instructions or products referred to in the content.